Heliyon 10 (2024) e27151

Contents lists available at ScienceDirect

Heliyon

journal homepage: www.cell.com/heliyon

Research article

Synergistic role of activated CD4$^+$ memory T cells and CXCL13 in augmenting cancer immunotherapy efficacy

Wenhao Ouyang [a,1], Qing Peng [a,1], Zijia Lai [b,1], Hong Huang [c], Zhenjun Huang [a], Xinxin Xie [a], Ruichong Lin [d], Zehua Wang [d], Herui Yao [a,**], Yunfang Yu [a,d,*]

[a] Guangdong Provincial Key Laboratory of Malignant Tumor Epigenetics and Gene Regulation, Department of Medicine Oncology, Sun Yat-sen Memorial Hospital, Sun Yat-sen University, Guangzhou, China
[b] Clinical Medicine College, Guangdong Medical University, Zhanjiang, China
[c] Clinical Medicine College, Guilin Medical University, Guilin, China
[d] Faculty of Medicine, Macau University of Science and Technology, Taipa, Macao, China

ARTICLE INFO

Keywords:
Activated CD4$^+$ memory T cells
Immunotherapy
CXCL13
Deep learning model

ABSTRACT

The development of immune checkpoint inhibitors (ICIs) has significantly advanced cancer treatment. However, their efficacy is not consistent across all patients, underscoring the need for personalized approaches. In this study, we examined the relationship between activated CD4$^+$ memory T cell expression and ICI responsiveness. A notable correlation was observed between increased activated CD4$^+$ memory T cell expression and better patient survival in various cohorts. Additionally, the chemokine CXCL13 was identified as a potential prognostic biomarker, with higher expression levels associated with improved outcomes. Further analysis highlighted CXCL13's role in influencing the Tumor Microenvironment, emphasizing its relevance in tumor immunity. Using these findings, we developed a deep learning model by the Multi-Layer Aggregation Graph Neural Network method. This model exhibited promise in predicting ICI treatment efficacy, suggesting its potential application in clinical practice.

1. Introduction

The advent of immune checkpoint inhibitors (ICIs) has ushered in a transformative phase in oncological treatments. Despite their promising potential, their effectiveness is restricted to a limited subset of cancer patients [1,2]. This discrepancy underscores an imperative for refined, patient-specific therapeutic strategies.

The tumor microenvironment (TME) represents a multifaceted environment populated by tumor cells, immune cells, and assorted components. Within this intricate landscape, tumors have developed strategies to evade immune detection. This evasion is precisely what ICIs target, aiming to bolster the body's natural defensive mechanisms against these malignancies [3]. At the heart of this complex interplay lies the CD4$^+$ T cell. Specifically, those CD4$^+$ T cells that produce CXCL13 take on a crucial role in sculpting the

* Corresponding author. Guangdong Provincial Key Laboratory of Malignant Tumor Epigenetics and Gene Regulation, Department of Medical Oncology, Sun Yat-sen Memorial Hospital, Sun Yat-sen University, No. 107 Yanjiang West Road, Guangzhou 510120, China.
** Corresponding author. Guangdong Provincial Key Laboratory of Malignant Tumor Epigenetics and Gene Regulation, Phase I Clinical Trial Center, Sun Yat-sen Memorial Hospital, Sun Yat-sen University, No. 107 Yanjiang West Road, Guangzhou 510120, China.
E-mail addresses: yaoherui@mail.sysu.edu.cn (H. Yao), yuyf9@mail.sysu.edu.cn (Y. Yu).
[1] Authors contributed equally to this work and should be considered co-first authors.

https://doi.org/10.1016/j.heliyon.2024.e27151
Received 5 September 2023; Received in revised form 13 February 2024; Accepted 26 February 2024
Available online 3 March 2024

TME, most notably by impacting the tertiary lymphoid structure (TLS) [4]. The significance of these cells goes beyond mere existence; their interactions, especially with dendritic cells, are instrumental in determining the success of immunotherapeutic interventions [5]. Furthermore, the contribution of $CD4^+$ memory T cells to the preservation of immunological memory is vital for both mounting potent defenses against tumors and preventing their re-emergence [6].

The pivotal role of $CD4^+$ T cells within the immunological framework is well-established. However, the intricate dynamics governing their differentiation and subsequent functional manifestations within the TME remain subjects of ongoing scholarly investigation. In the specific realm of colorectal cancer, emerging research underscores the significance of distinct subsets of CD4 TH1-like cells [7,8]. Notably, those cells manifesting elevated expression levels of CXCL13 are garnering attention for their potential as predictive biomarkers of responsiveness to Immune Checkpoint Inhibitor (ICI) therapies [9,10]. Complementing this, recent scientific endeavors have illuminated novel molecular pathways, with the IGFLR1/IGFL3 axis being a case in point [11]. The identification and exploration of such pathways not only enhance our molecular understanding but also signal potential therapeutic innovations in the ever-evolving landscape of cancer immunotherapy.

This study aimed to elucidate the differential roles of activated $CD4^+$ memory T cells and CXCL13 in the TME by examining their presence and effects across various tumor immunotherapy cohorts. By identifying distinctions between ICI-responsive and non-responsive groups, we strive to underscore the predictive significance of these markers. Leveraging the power of deep learning models, we further endeavor to unveil the potent predictive capability of activated $CD4^+$ memory T cells in gauging ICI treatment outcomes. This study holds the potential to introduce these cells as an invaluable tool for pre-treatment assessment in immunotherapy patients.

2. Results

In this study, a comprehensive analysis was conducted on a population comprising 681 patients at the individual patient level, employing rigorously validated mRNA and genomic data as stipulated by the TRIPOD guidelines. The graphical representation encapsulating the essence of this research can be found in Fig. 1. The focal demographic under scrutiny encompassed 436 patients

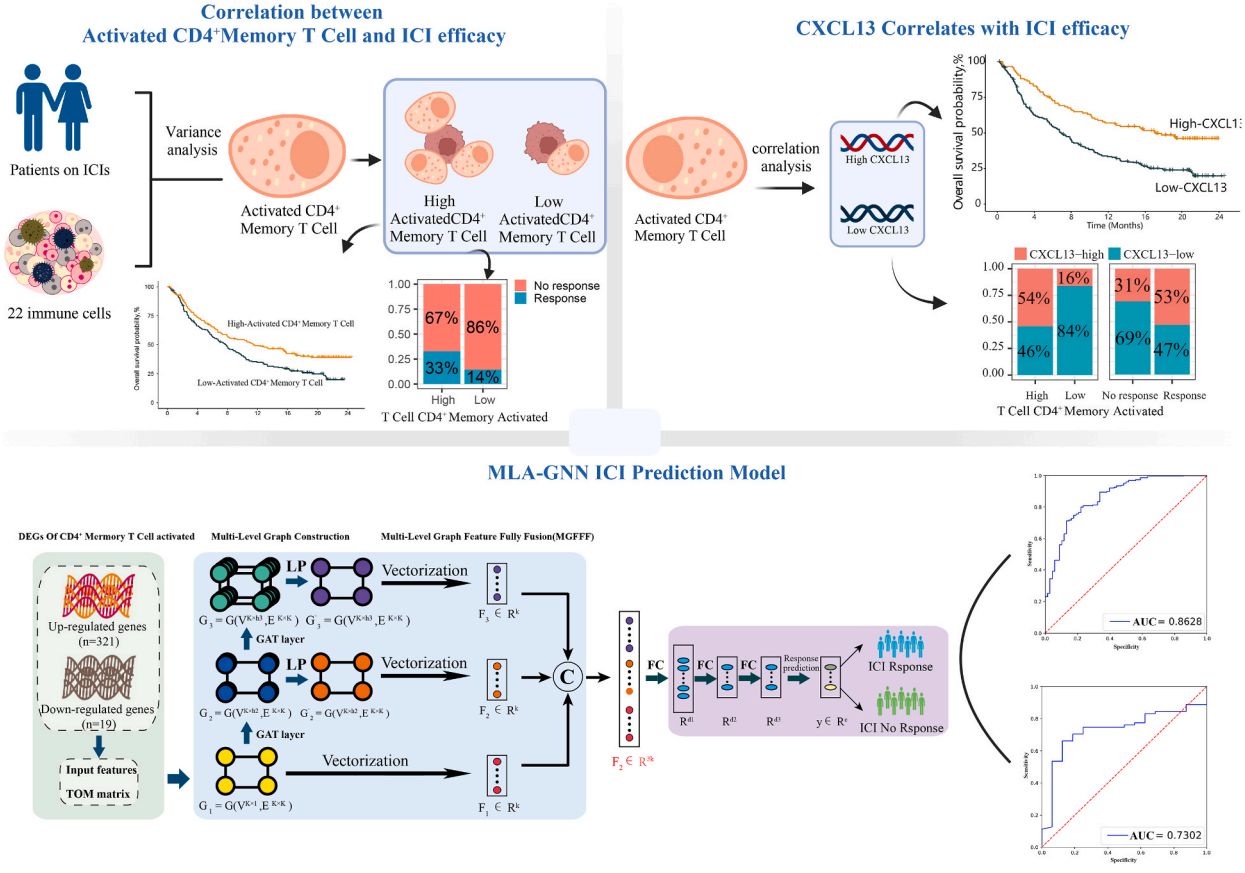

Fig. 1. Overview of the Study
This figure created with BioRender.com illustrates the comprehensive research workflow, divided into three main parts, focusing on the correlation between activated $CD4^+$ Memory T Cells and Immune Checkpoint Inhibitor (ICI) efficacy, the relationship of CXCL13 with ICI efficacy, and the proposed MLA-GNN ICI Prediction Model.

diagnosed with metastatic urothelial carcinoma from the IMvigor210 and GSE176307 cohorts, alongside an additional 115 patients afflicted with metastatic melanoma sourced from the GSE78220 and PRJEB23709 cohorts. Furthermore, from the GSE35640 dataset, we collected 65 melanoma patients who took part in two Phase II trials. Similarly, data from GSE91061 included information on 65 melanoma patients who received anti-PD-1 therapy. The clinical attributes of these patients have been summarized (Table 1).

2.1. Correlation between activated $CD4^+$ memory T Cell Expression and Immunotherapy Response

Initially, we explored the correlation between activated $CD4^+$ memory T cell expression and overall survival (OS) improvement in patients receiving Immune Checkpoint Inhibitors (ICIs) in the IMvigor210 Cohort. We observed a strong correlation ($P = 0.0025$, Hazard ratio = 0.668, 95%CI: 0.514–0.869) between increased expression of activated $CD4^+$ memory T cells and improved OS (Fig. 2A).

Furthermore, we conducted survival analyses on activated $CD4^+$ memory T cells in mUC-Cohort2 and Melanoma Cohort. Across all cohorts, higher expression levels of activated $CD4^+$ memory T cells were consistently associated with improved prognosis. Notably, mUC-Cohort2 exhibited a significant survival advantage ($P = 0.013$, Hazard Ratio = 0.441, 95% CI: 0.228–0.856) (Fig. 2B), and mUC-Cohort2 displayed a similar trend in progress-free survival ($P = 0.022$, Hazard Ratio = 0.539, 95% CI: 0.315–0.923) (Fig. 2C), and Melanoma Cohort demonstrated the most pronounced survival benefit ($P = 0.002$, Hazard Ratio = 0.320, 95% CI: 0.150–0.682) (Fig. 2D).

To further investigate the cellular composition, we employed the CIBERSORT algorithm to perform cell annotation on the IMvigor210 Cohort. Heatmaps were generated for the responsive and non-responsive groups. The results revealed significant differences in the abundance of activated $CD4^+$ Memory T Cells and Macrophages M1 between the responsive and non-responsive groups (Fig. 2E). To validate these findings, we conducted an analysis on an additional melanoma dataset (GSE35640+GSE91061), which confirmed the persistent differences in activated $CD4^+$ Memory T Cells between the responsive and non-responsive groups (Lower part of Fig. 2E).

In terms of treatment response, activated $CD4^+$ memory T cell expression was significantly higher (p-value <0.01) in patients who responded to ICIs compared to non-responders (Fig. 2F). Furthermore, the high-expression group of activated $CD4^+$ memory T cells demonstrated a substantially higher objective response rate (ORR) than the low-expression group (33% vs. 14%) (Fig. 2G).

These results highlight the significance of activated $CD4^+$ memory T cells in the context of immunotherapy and their potential as a biomarker for treatment response prediction. Further research is warranted to elucidate the underlying mechanisms by which activated $CD4^+$ memory T cells influence the tumor immune microenvironment and interact with immune checkpoint molecules.

2.2. Associations of activated $CD4^+$ memory T cell with immune phenotype

We aimed to elucidate the critical role of activated $CD4^+$ memory T cells in determining the responsiveness to immune checkpoint inhibitors (ICIs) within the Tumor Immune Microenvironment (TIME). We evaluated the association between activated $CD4^+$ memory T cells and immune phenotypes in the IMvigor210 trial. Based on the three previously defined immune phenotypes [23] revealed that activated $CD4^+$ memory T cells exhibited the highest expression in the immune-inflamed phenotype and the lowest expression in the

Table 1
The clinical characteristics of the patients were included in this study.

Cohorts	IMvigor210	GSE176307	GSE78220	PRJEB23709	GSE35640	GSE91061
Cancer type	metastatic urothelial carcinoma	metastatic urothelial carcinoma	metastatic melanoma	metastatic melanoma	metastatic melanoma	metastatic melanoma
Number of patients	348	88	27	88	65	65
Age (median, SD), years	–	70.50 ± 10.26	61.00 ± 15.17	57.00 ± 12.50		–
Gender						
Male	272 (78.2%)	55 (62.5%)	19 (70.4%)	53 (60.2%)	–	–
Female	76 (21.8%)	33 (37.5%)	8 (29.6%)	35 (39.8%)	–	–
Median Overall Survival Time, Months	8.05 ± 7.65	5.72 ± 6.88	14.43 ± 10.00	20.02 ± 7.26	–	–
Median Progression-Free Survival Time, Months	–	2.07 ± 5.38	–	16.92 ± 9.21	–	–
Survival Status						
Alive	116 (33.3%)	31 (35.2%)	15 (55.6%)	71 (80.7%)	–	–
Deceased	232 (66.7%)	57 (64.8%)	12 (44.4%)	17 (19.3%)	–	–
Response						
CR/PR	68	16	14	56	22	13
SD/PD	230	71	13	32	34	43
NA	50	1	–	–	9	2
Stage						
I	118	–	–	–	–	–
II	95	–	–	–	–	–
III	69	–	–	–	–	–
IV	66	–	–	–	–	–
Therapy	anti-PD-L1	anti-PD-1/PD-L1	anti-PD-1	anti-CTLA4 or anti-PD-1	anti-PD-1	anti-PD-1

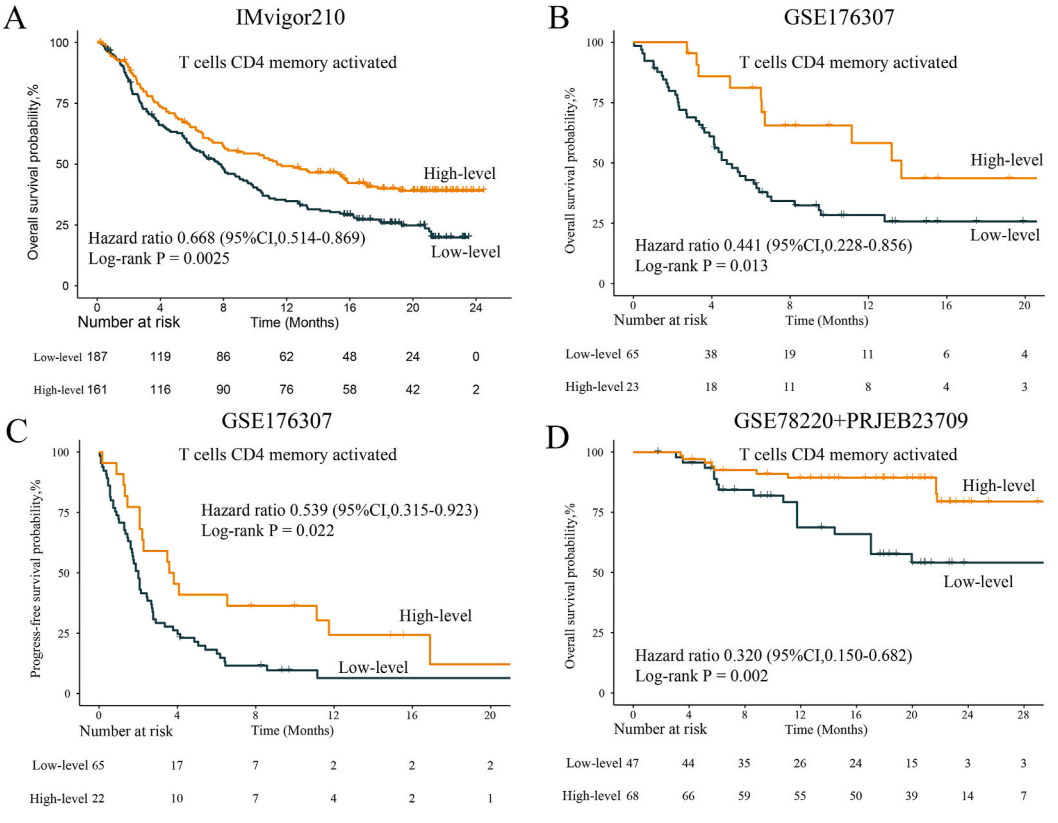

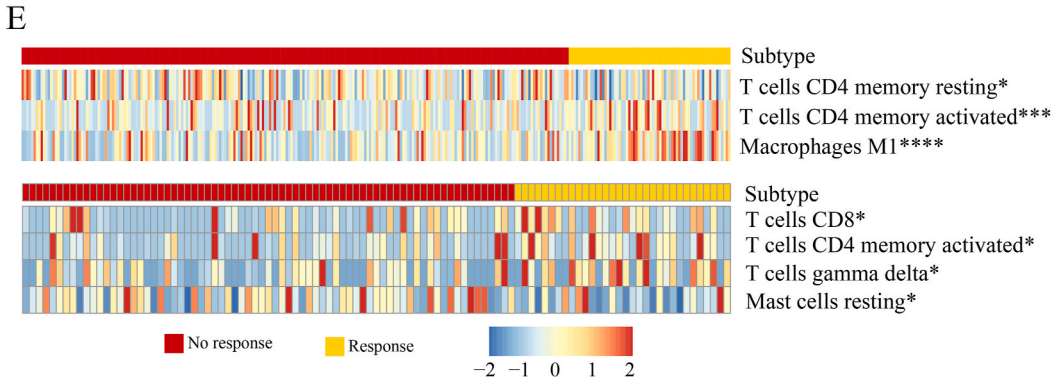

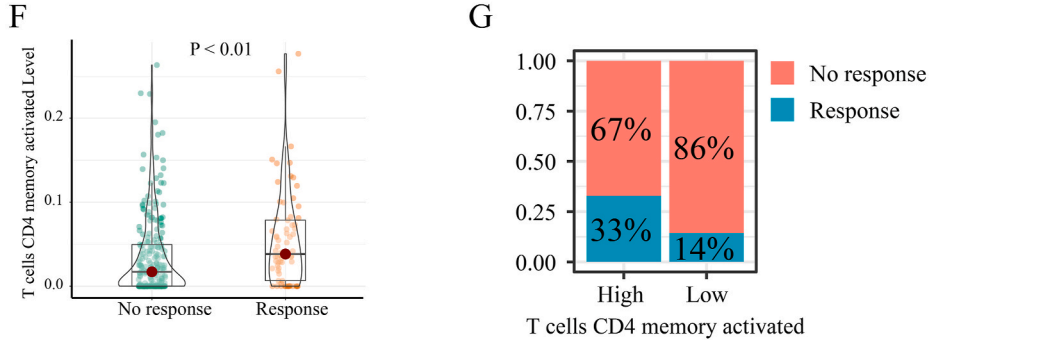

(caption on next page)

Fig. 2. Correlation between CD4$^+$ Memory T Cell Expression and Immunotherapy Response (A) Overall Survival Analysis of Activated CD4$^+$ Memory T Cells in IMvigor210 Cohort. (B) Overall Survival Analysis of Activated CD4$^+$ Memory T Cells in mUC-Cohort2 (GSE176307). (C) Progress-free Survival Analysis of Activated CD4$^+$ Memory T Cells in mUC-Cohort2 (GSE176307). (D) Overall Survival Analysis of Activated CD4$^+$ Memory T Cells in Melanoma Cohort (GSE78220+PRJEB23709). (E) Distribution Heatmap of Immune Cell Populations in Responders and Non-responders. (F) Expression Levels of Activated CD4$^+$ Memory T Cells in Responders and Non-responders. (G) Distribution of Objective Response Rate in Activated CD4$^+$ Memory T Cells High and Low Expression Groups.

immune-desert phenotype ($P < 0.01$) (Fig. 3A). Moreover, PD-L1 expression level on infiltrating immune cells (ICs) positively correlated with activated CD4$^+$ memory T cells expression levels ($P < 0.001$) (Fig. 3B). The expression level of activated CD4$^+$ memory T cells lacked a significant relationship with PD-L1 expression level on infiltrating tumor cells (TCs) (Fig. 3C). By employing four distinct immune phenotypes based on long non-coding RNA (lncRNA) and tumor-specific cytotoxic T lymphocytes (CTL) combinations [24], we found that activated CD4$^+$ memory T cell expression was significantly higher in the immune-active phenotype compared to immune-excluded, immune-desert, and immune-dysfunction phenotypes (all P-values <0.05) (Fig. 3D).To investigate the role of activated CD4$^+$ memory T cells in determining the crucial TIME (Tumor Immune Microenvironment) for ICI responsiveness, we examined the association between activated CD4$^+$ memory T cells and immune checkpoint molecules in the IMvigor210 trial. Our findings revealed that patients with elevated PD-L1 expression exhibited higher levels of activated CD4$^+$ memory T cell expression. Additionally, we identified a co-expression pattern between activated CD4$^+$ memory T cells and other immune checkpoint molecules, including CTLA4, PD-1, IDO1, and LAG3. Compared to the low-expression group, the high-expression group of activated CD4$^+$ memory T cells showed significantly higher expression levels of these immune checkpoint molecules (Fig. 3E).

Moreover, our data indicated a positive correlation between the expression levels of these immune checkpoint molecules and activated CD4$^+$ memory T cells (Fig. 3F). This finding suggests a possible synergistic effect in modulating the tumor immune response when these molecules are co-expressed with activated CD4$^+$ memory T cells. To validate the robustness of our observations, we replicated the analysis in two additional immunotherapy cohorts, and the results were consistent with those from the IMvigor210 trial (Fig. 3G–J).

The association of activated CD4$^+$ memory T cells with immune phenotypes and IC immune scores suggests their involvement in shaping the immune landscape and response to ICIs. Further investigations are warranted to decipher the specific mechanisms by which activated CD4$^+$ memory T cells modulate the immune response and explore their potential as predictive biomarkers for ICI treatment outcomes.

2.3. Identification of Key Biomarkers associated with ICI responsiveness

In this study, we aimed to provide a comprehensive description of the heterogeneity of activated CD4$^+$ memory T cells within the Tumor Immune Microenvironment (TIME). To achieve this, we conducted a thorough analysis of the IMvigor210 trial, focusing on identifying key marker genes highly correlated with activated CD4$^+$ memory T cell infiltration and responsiveness to Immune Checkpoint Inhibitors (ICIs).

Initially, we stratified the samples into high and low expression groups based on CD4 expression levels and performed a differential gene expression analysis. This analysis led to the identification of 19 downregulated genes and 321 upregulated genes (Fig. 4A).

To gain insights into the functional implications of these differentially expressed genes (DEGs), we conducted Gene Ontology (GO) pathway enrichment analysis. The results revealed significant associations of these DEGs with immune processes, including leukocyte-mediated immunity, cell-cell adhesion, activated T cell regulation, immune receptor activity, immunological synapse, and MHC protein complex (Fig. 4B). Furthermore, KEGG pathway enrichment analysis highlighted enrichment in cell adhesion molecules and cytokine-cytokine receptor interaction processes (Fig. 4C).

Next, we focused on identifying genes that could distinguish immunotherapy responders from non-responders and genes that differed significantly between the high activated CD4$^+$ memory T cell and low activated CD4$^+$ memory T cell groups. Among these, 9 genes (CXCL10, ALDH1L1, CXCL13, ANXA10, AREG, UBD, CXCL9, CA12, KLRC2) were found to be overlapping DEGs (Fig. 4D). To assess the relationship of activated CD4$^+$ memory T cells with these intersecting genes, we analyzed their correlation (Fig. 4E). Notably, CXCL13 exhibited the highest correlation and was identified as the most critical gene for subsequent analyses. Additionally, CXCL9, KLRC2, UBD, CXCL10, and AREG showed positive correlations, while CA12, ALDH1L1, and ANXA10 showed negative correlations.

CXCL13 is a chemokine that is highly expressed in germinal center-associated helper T cells, and it plays a crucial role in facilitating B cell entry into the germinal center. We observed that among patients with high CD4 expression, 54% of them also showed high CXCL13 expression, whereas in the CD4 low-expression group, only 16% exhibited high CXCL13 expression. Meanwhile, in the non-responder group there were 69% of patients with low CXCL13 expression and 53% of patients exhibited high CXCL13 expression in the responder group (Fig. 4F). Likewise, CXCL13 expression was significantly higher ($P = 0.01$) in patients who responded to ICIs compared to non-responders (Fig. 4G).

To explore its potential as a predictive biomarker for immune checkpoint inhibitor (ICI) therapy efficacy, we stratified patients based on CXCL13 expression levels and examined its impact on overall survival using data from the IMvigor210 trial. The results revealed that patients with high CXCL13 expression had a significantly better prognosis ($P < 0.0001$, Hazard ratio = 0.498, 95% CI: 0.371–0.668) (Fig. 4H). The same conclusion is validated for mUC-Cohort2 in overall survival ($P < 0.001$, Hazard ratio = 0.367, 95% CI: 0.213–0.633) (Fig. 4I). mUC-Cohort2 in progress-free survival was also used to validate the conclusions above ($P < 0.001$, Hazard

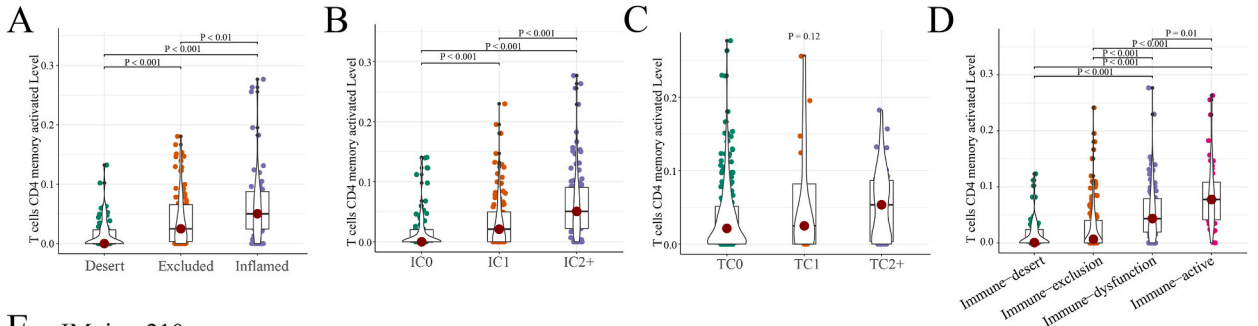

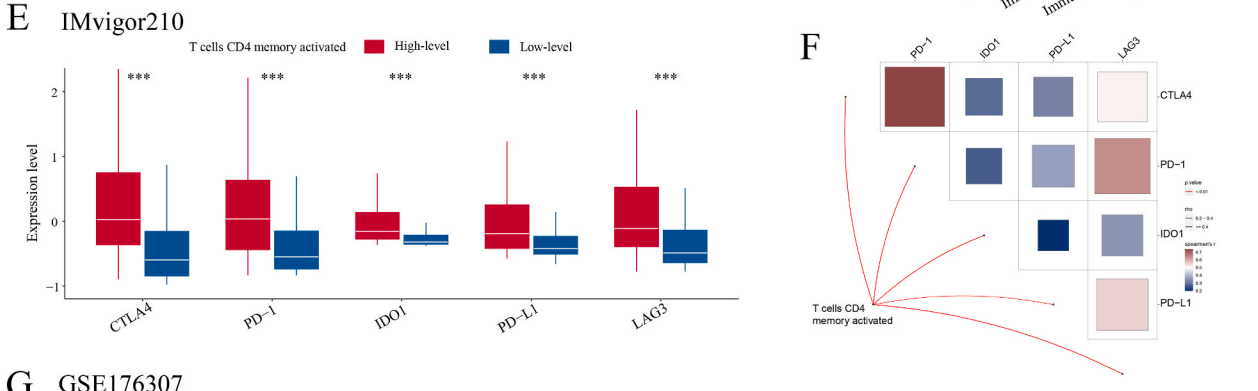

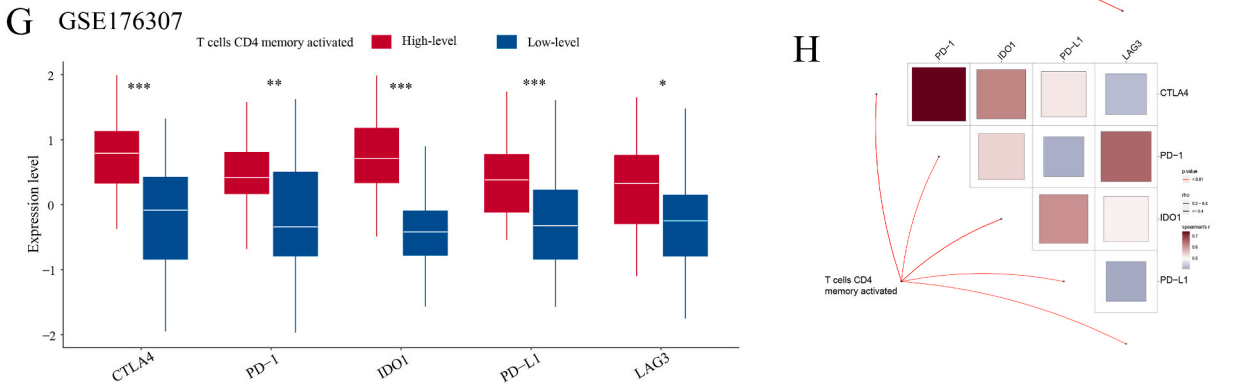

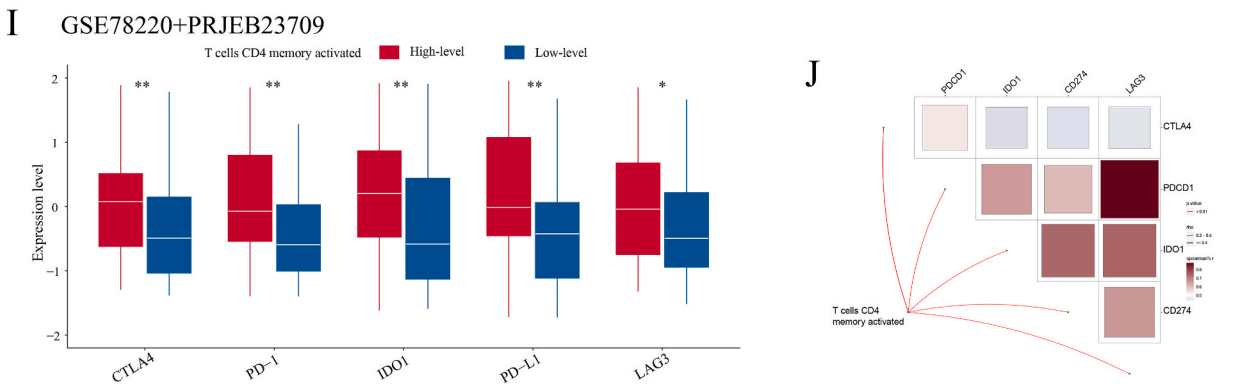

(caption on next page)

Fig. 3. Activated CD4$^+$ Memory T Cells in Immunophenotype and Immune Checkpoint Relationships (A) Difference of Activated CD4$^+$ Memory T Cell Expression with Immune Subtypes. (B) Difference of Activated CD4$^+$ Memory T Cell Expression with PD-L1 level of Immune Cells (IC). (C) Difference of Activated CD4$^+$ Memory T Cell Expression with PD-L1 level of Tumor Cells (TC). (D) Difference of Activated CD4$^+$ Memory T Cell Expression with Related lncRNA Subtypes. (E) Difference between Activated CD4$^+$ Memory T Cell Expression and Immune Checkpoints in the IMvigor210 Cohort. (F) Correlation Analysis between Activated CD4$^+$ Memory T Cells and Immune Checkpoints in the IMvigor210 Cohort. (G) Difference between Activated CD4$^+$ Memory T Cell Expression and Immune Checkpoints in mUC-Cohort2 (GSE176307). (H) Correlation Analysis between Activated CD4$^+$ Memory T Cells and Immune Checkpoints in mUC-Cohort2 (GSE176307). (I) Difference between Activated CD4$^+$ Memory T Cell Expression and Immune Checkpoints in the Melanoma Cohort (GSE78220+PRJEB23709). (J) Difference Analysis between Activated CD4$^+$ Memory T Cells and Immune Checkpoints in the Melanoma Cohort (GSE78220+PRJEB23709).

ratio = 0.522, 95%CI: 0.324–0.843) (Fig. 4J).

By conducting these analyses, we have gained valuable insights into the heterogeneity of activated CD4$^+$ memory T cells in the Tumor Immune Microenvironment. The identified marker genes and their correlations may have important implications for understanding immune responses and guiding the development of targeted immunotherapies for cancer treatment.

3. Exploring the impact of CXCL13 on the tumor immune microenvironment

To gain deeper insights into the potential impact of CXCL13 on the tumor immune microenvironment (TIME), we conducted a comparative analysis using data from the IMvigor210 trial. Specifically, we compared the gene expression profiles between the high CXCL13 expression group and the low CXCL13 expression group. Our analysis revealed 320 downregulated genes and 850 upregulated genes in the high CXCL13 expression group (Fig. 5A).

Moreover, the Gene Ontology (GO) pathway enrichment analysis showed a significant correlation between these differentially expressed genes (DEGs) and immune processes, with functional enrichment resembling that of activated CD4$^+$ memory T cells (Fig. 5B). Additionally, the Kyoto Encyclopedia of Genes and Genomes (KEGG) enrichment analysis revealed enrichment in the cytokine-cytokine receptor interaction process and the chemokine signaling pathway (Fig. 5C).

To further investigate the cellular composition and immune microenvironment scores, we employed the CIBERSORT algorithm. The comprehensive heatmap (Fig. 5D) illustrated a higher proportion of cells with elevated immune checkpoint levels, activated CD4 memory T cells, and memory B cells in the high CXCL13 expression group. Additionally, the StromalScore and ImmuneScore were significantly higher in the high CXCL13 expression group compared to the low expression group, indicating increased infiltration of stromal and immune cells in the TIME. Notably, the high CXCL13 expression group exhibited a substantial presence of M1 macrophages.

Our investigation also delved into the relationship between CXCL13 expression levels and immune subtypes in tumors. The results indicated a significant association between high CXCL13 expression and the inflammatory subtype of tumors within the tumor immune three-subtype classification ($P < 0.01$) (Fig. 5E). Additionally, PD-L1 expression status on infiltrating immune cells (ICs) were found to positively correlate with CXCL13 expression levels ($P < 0.001$) (Fig. 5F). However, there was no significant relationship between the expression level of CXCL13 and PD-L1 expression status on infiltrating immune cells ($P = 0.12$) (Fig. 5G). These results suggest that CXCL13 may be more correlated with the immune checkpoint score expressed by immune cells than that expressed by tumors. Utilizing four distinct immune phenotypes, which were based on combinations of long non-coding RNA (lncRNA) and tumor-specific cytotoxic T lymphocytes (CTL) [24], CXCL13 expression was significantly higher in the immune-active phenotype compared to the immune-excluded, immune-desert, and immune-dysfunction phenotypes ($P < 0.05$) (Fig. 5H).This finding suggests a crucial role for CXCL13 in shaping the tumor immune microenvironment and promoting immune responses.

Furthermore, we noted a positive correlation between CXCL13 expression and the abundance of immune checkpoints (Fig. 5I and J). This discovery indicates a potential link between CXCL13 expression and immune checkpoint regulation, with potential implications for the responsiveness to immune checkpoint inhibitor (ICI) therapy. Understanding the role of CXCL13 in the tumor immune microenvironment could contribute to the development of more effective and personalized immunotherapeutic strategies.

3.1. A novel predictive model for ICIs Treatment Prognosis with MLA-GNN models

In our prior research, we have gained valuable insights into the consistent correlation between elevated expression levels of activated CD4 memory T cells and CXCL13 and improved prognosis in the context of Immune Checkpoint Inhibitors (ICIs) therapy. Building upon this knowledge, we have successfully developed a pioneering predictive model for the clinical prognosis of ICIs treatment. This model leverages activated CD4 memory T cell-related genes and employs the MLA-GNN (Multi-Layer Aggregation Graph Neural Network) model, as illustrated in Fig. 6A.

The newly developed model demonstrates promising predictive capabilities for the Objective Response Rate (ORR) in patients undergoing ICIs therapy. To assess its performance, we employed the IMvigor210 Cohort the training group, consisting of 298 individuals, and the mUC-Cohort2 as the test group, consisting of 87 individuals, resulting in AUC values of 0.8628 in IMvigor210 Cohort (Fig. 6B) and 0.7302 in mUC-Cohort2 (Fig. 6C), respectively. These results highlight the potential of our innovative model in effectively predicting the response to ICIs treatment and enhancing patient outcomes.

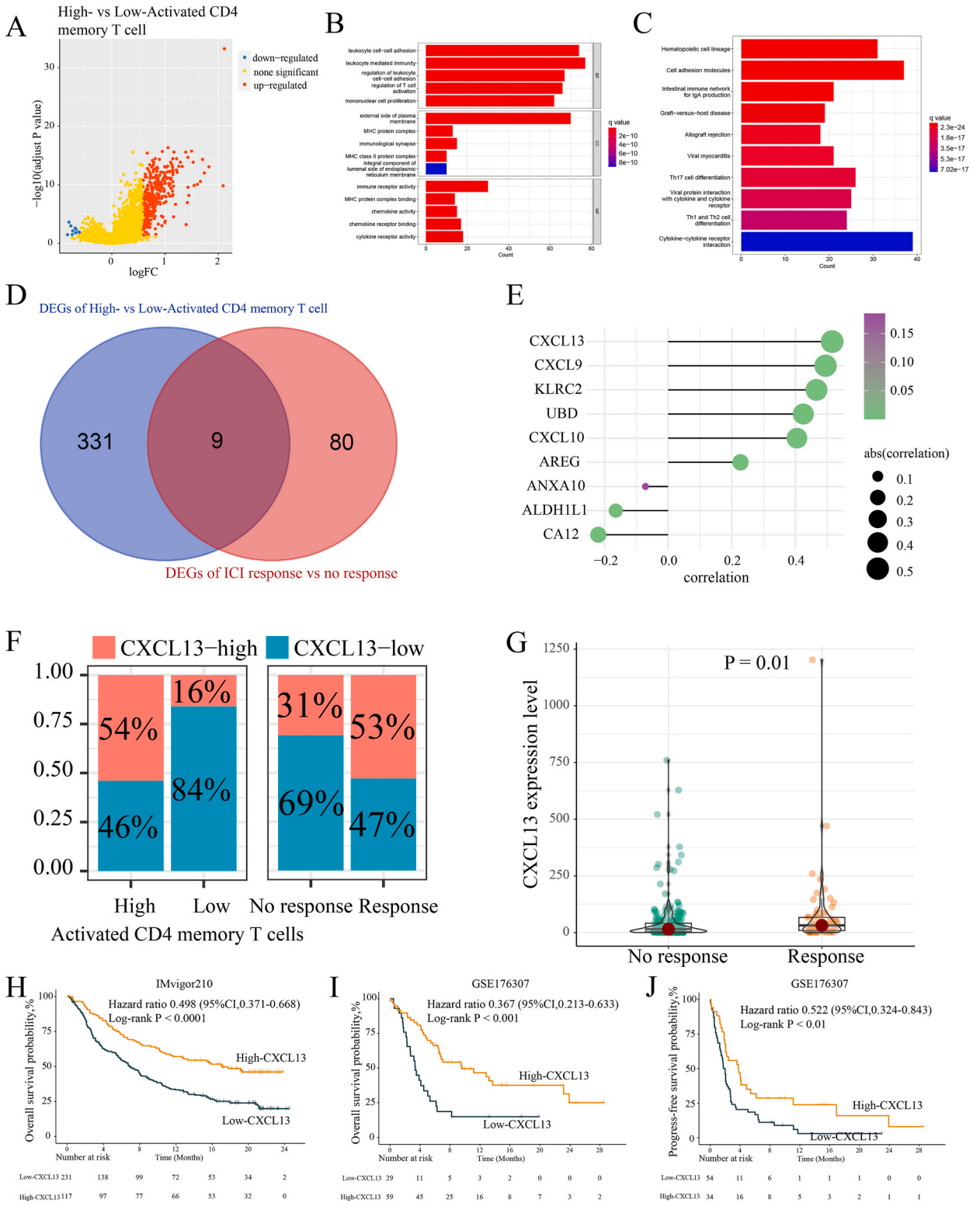

(caption on next page)

Fig. 4. CXCL13 as the Key Biomarker of Activated $CD4^+$ Memory T Cells (A) Differentially expressed genes between high and low Activated $CD4^+$ Memory T Cell level groups. (B) GO analysis of differentially expressed genes between groups with high and low levels of Activated $CD4^+$ Memory T Cells. (C) KEGG analysis of differentially expressed genes between groups with high and low levels of Activated $CD4^+$ Memory T Cells. (D) The intersection of differentially expressed genes between groups with high and low levels of Activated $CD4^+$ Memory T Cells and groups responsive and non-responsive to ICIs treatment. (E) Differential expressed gene between high and low Activated $CD4^+$ Memory T Cell levels groups and correlation analysis with Activated $CD4^+$ Memory T Cell. (F) The proportion of patients with high and low CXCL13 levels in relation to the high and low activated $CD4^+$ memory T cell groups and the responsiveness to ICI treatment. (G) Difference in CXCL13 expression between ICI treatment responsive and non-responsive groups (H) The difference in OS between the high and low CXCL13 level groups in the IMvigor210 cohort. (I) The difference in OS between the high and low CXCL13 level groups in the mUC-Cohort2 (GSE176307). (J) The difference in PFS between the high and low CXCL13 level groups in the mUC-Cohort2 (GSE176307).

4. Discussion

This study elucidated the paramount importance of activated $CD4^+$ memory T cells in mediating immunotherapy outcomes. Through rigorous analysis, we discerned a robust association between augmented expression of activated $CD4^+$ memory T cells and enhanced clinical outcomes in patients treated with immune checkpoint inhibitors (ICIs). Notably, the gene CXCL13 emerged as a salient molecular marker, showing a significant correlation with the expression profiles of activated $CD4^+$ memory T cells and ICI therapeutic responsiveness. Upon intricate examination of the tumor immune microenvironment, we observed that elevated CXCL13 expression was concomitant with heightened immune activity. Importantly, leveraging advanced deep learning algorithm, we constructed a prognostic model predicated upon the differentially expressed genes from activated $CD4^+$ memory T cells. This model exhibited exceptional efficacy in predicting ICI therapeutic responses. In total, our data robustly support the paramount prognostic potential of both activated $CD4^+$ memory T cells and our bespoke model.

Recent advancements in immunotherapy have elucidated the significance of various cellular and molecular markers in shaping therapeutic outcomes. Traditionally, the spotlight has been cast upon $CD8^+$ T cells, owing to their primary effector role in tumor eradication [25–28]. Nonetheless, our seminal research accentuates the paramount role of activated $CD4^+$ memory T cells within the tumor microenvironment. This pivotal realization originated from the observation that $CD4^+$ T cells in melanoma cells could discern cancer antigens, instigating robust, long-term immunity. Such immunological responses were subsequently pinpointed across a spectrum of cancer types.

In a compelling turn of events, an examination of circulating T cells from patients administered ipilimumab (anti-CTLA-4) unveiled a correlation: a surge in $CD4^+$ T cells was concomitant with enhanced survival outcomes and clinical efficacy [29]. Historically delegated a mere helper function in immunity, burgeoning evidence now unveils the direct cytotoxic prowess of $CD4^+$ T cells [30]. These cells, in the throes of acute and chronic viral onslaughts, target and eradicate cells by recognizing antigens presented on MHC Class II molecules [31]. Such cytotoxic $CD4^+$ T cells, identified in various human malignancies, portend an auspicious avenue for their incorporation into immunotherapeutic regimens. T cell-mediated responses in tumor immunology are undeniably paramount. Notably, activated $CD4^+$ T cells can augment cytotoxic T lymphocyte (CTL) reactions, serve as effector cells, and, intriguingly, manifest inhibitory propensities via the $CD4^+$ $CD25^+$ regulatory subset. Previous endeavors have underscored the enduring nature of memory $CD4^+$ T cells, borne from infection or immunization, which flourish upon subsequent antigen encounters even in the absence of adjuvants [32,33]. Yet, the intricacies surrounding the presence and role of activated $CD4^+$ memory T cells within tumors remain enigmatic. This amplifies the gravity of our discovery, establishing a positive correlation between these cells and cancer survival, intricately linked with the prowess of ICI therapies.

CXCL13's emergence as a pivotal molecular marker in the oncology domain offers novel trajectories for research. Historically, this chemokine has been recognized for its role in orchestrating secondary lymphoid structures and recruiting B cells [34,35]. A discernible association of its elevated expression with amplified immune activity within the tumor microenvironment potentially underscores its significance in creating conditions favorable for Immune Checkpoint Inhibitor (ICI) effectiveness. The intricate relationship between heightened CXCL13 expression and the vigor of activated $CD4^+$ memory T cells posits a conceivable feedback mechanism. Upon their activation, these T cells might either synthesize or induce other immune cells to release CXCL13, thereby amplifying the overarching immune response. Recent investigations have identified the presence of CXCL13-expressing $CD8^+$ and $CD4^+$ T cell subsets within TNBC tumors [36]. Notably, these $CXCL13^+$ T cells demonstrate substantial expansion post-combinatorial treatments and bear a close association with tumor reactivity. Further empirical data reinforces the correlation between $CXCL13^+$ T cells and the efficacy of PD-L1 blockade therapy.

Another independent study found that the majority of high-grade serous ovarian cancer patients exhibited a limited response to immune checkpoint blockade, with the underlying reasons yet to be fully understood. Given the rejuvenated vitality of follicular cytotoxic $CXCR5^+$ $CD8^+$ T cells upon tumor immune checkpoint blockade, elevated CXCL13 expression within the tumor was found to denote a more immunogenically active microenvironment, potentially heralding an extended patient survival [37]. Additionally, $CXCL13^+$ T cells have been identified to execute crucial antitumor functions via interaction with dendritic cells (DC), cementing their importance for antitumor responses with anti-PD-1 treatments [5]. Our findings largely concur with previous research, elucidating that elevated CXCL13 expression correlates positively with favorable prognoses in tumor patients under ICIs treatment. Furthermore, a direct correlation has been discerned between CXCL13 and the infiltration extent of activated memory $CD4^+$ T cells. Mechanistically, within the tumor milieu, the expression of CXCL13 might be a response to specific stimuli, such as inflammation or other immune-activating factors [5]. This unique environment might foster the activation and proliferation of CD4 memory T cells [38]. Alternatively, the upsurge in CXCL13 might cause an influx of T cells and B cells to lymph nodes or the tumor microenvironment,

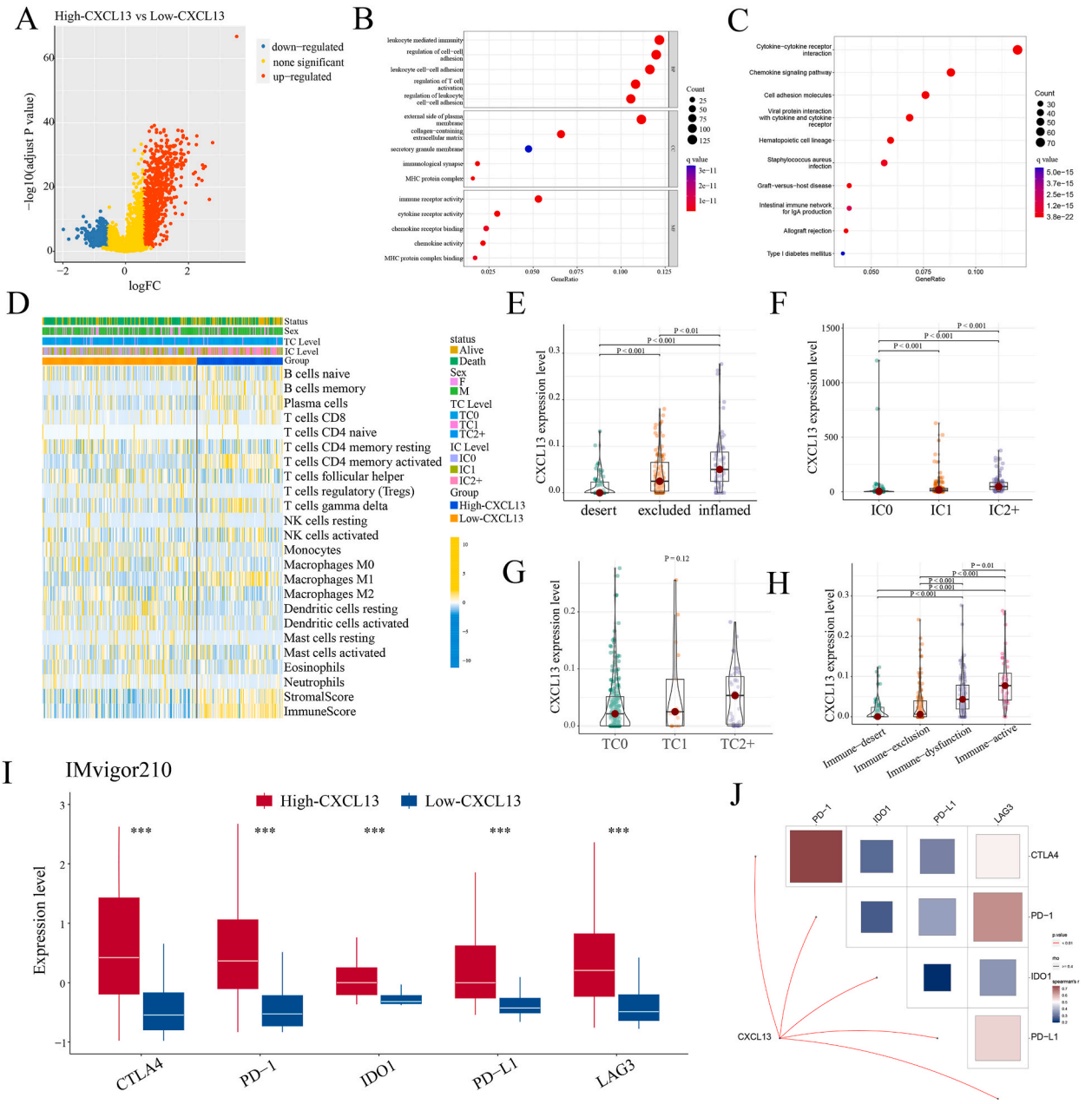

Fig. 5. CXCL13 in Immunophenotype and ICIs Efficacy. (A) Differentially expressed genes between high and low CXCL13 level groups. (B) GO analysis of differentially expressed genes between groups with high and low levels of CXCL13. (C) KEGG analysis of differentially expressed genes between groups with high and low levels of CXCL13. (D) Difference in immune cell infiltration between groups with high and low CXCL13 levels. (E) Difference of CXCL13 Expression among Immune Subtypes. (F) Difference of CXCL13 Expression among PD-L1 level of Immune Cells (IC) (G) Difference of CXCL13 Expression among PD-L1 level of Tumor Cells (TC) (H) Difference of CXCL13 Expression among Immune Related lncRNA Subtypes. (I) Difference between CXCL13 Expression and Immune Checkpoints in the IMvigor210 Cohort. (J) Correlation between CXCL13 Expression and Immune Checkpoints in the IMvigor210 Cohort.

amplifying antigen presentation, immune cell interplay, and the overall immune response. In essence, CXCL13 may be paramount in modulating immune responses and, consequently, tumor reactivity to ICIs.

Leveraging artificial intelligence in biomedical research, especially deep learning, has brought forth a paradigm shift, enabling the development of cutting-edge prognostic tools. Our model, built upon deep learning methodologies, extrapolates the differentially expressed genes of activated $CD4^+$ memory T cells, representing a confluence of molecular biology and computational prowess. In previous studies [39–44], other researchers have mostly used machine learning models to predict cancer immunotherapy effects, and the results are encouraging, but in our study, based on Activated $CD4^+$ Memory T Cells related genes combined with a deep learning

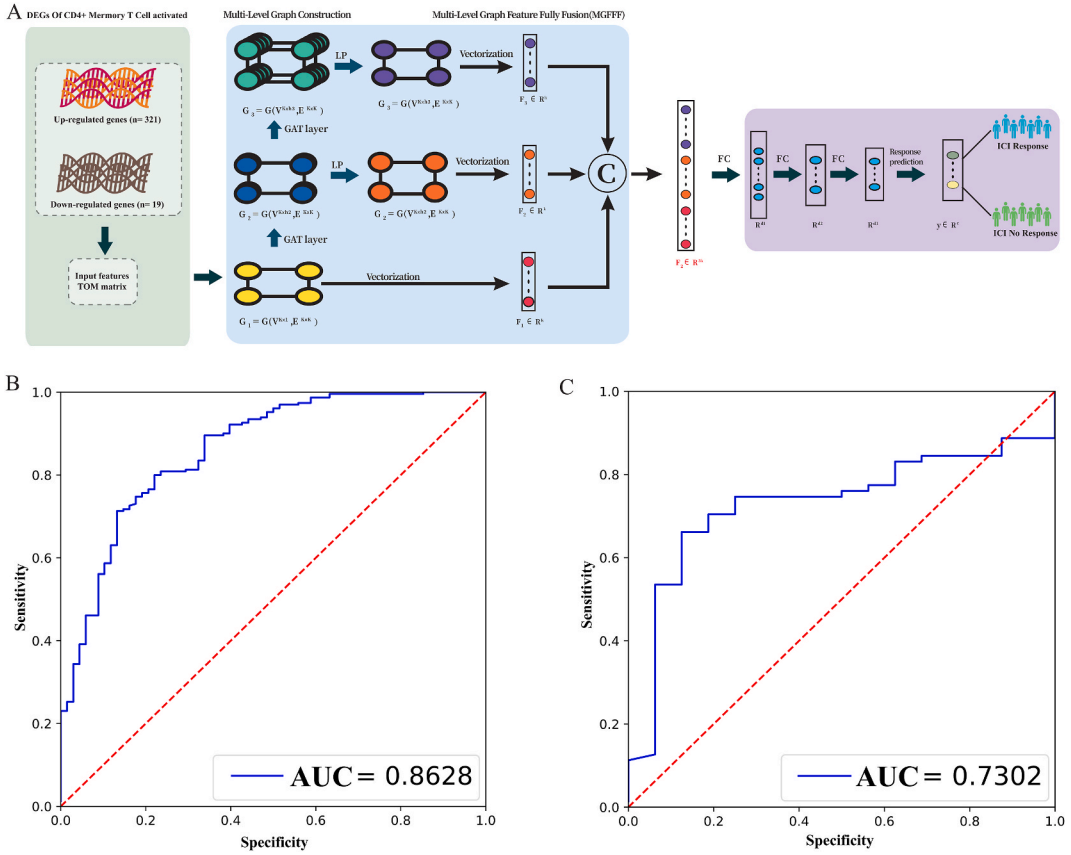

Fig. 6. Predictive Model for ICIs Treatment Prognosis with MLA-GNN Models (A) MLA-GNN Algorithm Workflow (B) ROC Curve for the IMvigor210 Cohort. (C) ROC Curve for the mUC-Cohort2 (GSE176307).

model, there is a higher prediction of ICI treatment effects. The demonstrated ability of our model to predict ICI responses is instrumental for clinicians, allowing for refined, individualized therapeutic decisions in an era increasingly moving towards personalized medicine.

Historically, the promise of deep learning in oncological prognosis has been illustrated in several studies. For instance, multi-modal deep learning models were formulated using pathological imagery from 14 distinct tumor types, combined with their matched genomic data [45]. Such an integrative approach paints a comprehensive picture, correlating histological and molecular features, thereby offering a detailed perspective into cancer patient risk and prognosis. Additionally, a recent exploration introduced a weakly supervised deep learning framework explicitly designed for prognostic predictions in HCC patients [46]. Utilizing digitized pathological images, this framework has revealed specific prognostic features, which are encapsulated within the TRS formula and can be visualized using heatmaps, emphasizing the potential relationship between tumor immune infiltration and its impact on microvessel formation, suggesting possible repercussions on the survival rates of HCC patients.

The imperative to delve deep into the tumor immune microenvironment arises from its pivotal role in shaping the interactions between malignancies and the patient's immune response. While biomarkers are gaining traction as tools to gauge the efficacy and predict side-effects of immunotherapies, their solitary use has shown limitations. The overarching challenge remains identifying a singular predictive biomarker capable of efficiently pinpointing patients who would most benefit from the treatment. This existing gap underscores the value and urgency of our work, emphasizing the need to amalgamate deep learning into the realm of oncological prognosis and prediction.

In conclusion, this study delineated the pivotal role of activated $CD4^+$ memory T cells and the chemokine CXCL13 within the Tumor Immune Microenvironment in predicting the efficacy of Immune Checkpoint Inhibitors treatment. Through multiple cohorts and rigorous analyses, we observed consistent correlations between elevated expressions of these markers and improved patient prognosis. Notably, utilizing these insights, we introduced an innovative MLA-GNN deep learning predictive model that showcased remarkable potential in forecasting treatment response. Our findings underscore the promise of personalized immunotherapy strategies, establishing the groundwork for enhanced therapeutic outcomes in oncological care.

5. Materials and methods

5.1. Study design

The study used data from 348 metastatic urothelial carcinoma (mUC) patients treated with the PD-L1 inhibitor atezolizumab from IMvigor210 [12]. Another set involved 88 mUC patients from GSE176307 [13] who received anti-PD1/PD-L1 therapy as well, which was named as the 'mUC-Cohort2′, as the survival verification cohorts. For the pre-treatment melanoma group on anti-PD-1 therapy, we sourced from GSE78220 [14] with 27 patients. 88 patients with metastatic melanoma who were treated anti-PD-1 or combined with anti-CTLA-4 were from PRJEB23709 [15]. These two cohorts were comprised as the 'Melanoma Cohort' as the survival verification cohorts. Additionally, 130 melanoma patients who underwent anti-PD-1 treatment, were collected from the GSE35640 and GSE91061 contributed data.

The main objective is to investigate the impact of ICIs on cancer patients' outcomes and their response to treatment. Specifically, patients will be categorized into two groups based on their response to ICIs: the "Responder Group" comprising complete and partial responses, and the "Non-Responder Group" comprising stable disease and disease progression.

5.2. Immune cell proportions

By leveraging the 'CIBERSORT' R package [16], we ascertained the proportions of 22 distinct immune cell types present in each sample. The full reference for the LM22 gene expression signature matrix can be found in (Supplementary Table 1). These include naive B cells, Bm, plasma cells, $CD8^+$ T cells, naive $CD4^+$ T cells, resting $CD4^+$ memory T cells, activated $CD4^+$ memory T cells, Tfh, Tregs, γδT, resting and activated natural killer cells, monocytes, macrophages (M0, M1, M2), dendritic cells (both resting and activated DC), resting mast cells, activated mast cells, eosinophils, and neutrophils.

5.3. Immune subsets and phenotypes

The immune phenotype within the IMvigor210 dataset includes three distinct subtypes: inflammatory, exclusionary, and desert immune [17]. Specifically, the immune desert subtype is characterized by the absence of immune cells, resulting in a complete lack of immune response against the tumor. Conversely, the immune-exclusionary subtype exhibits an immune response, but is populated by peripherally invading T cells that are unable to fully suppress the tumor. In contrast, the inflammatory subtype demonstrates an active immune response characterized by the presence of inflammatory myeloid cells and activated $CD8^+$ T cells within the tumor microenvironment.

In addition, the assessment of PD-L1 expression status on infiltrating immune cells (ICs) and tumor cells (TCs) [18,19] in the tumor microenvironment, is defined based on the percentage of PD-L1-positive immune cells as follows TC0 or IC0, $<1\%$; TC1 or IC1, $\geq 1\%$ but $<5\%$; TC2+ or IC2+ ($\geq 5\%$).

Moreover, in our previous study [24], we used signatures of long non-coding RNAs (lncRNAs) and cytotoxic T lymphocyte (CTL) infiltration to delineate four distinct immune classes in the context of clinical cancer immunotherapy. Specifically, patients classified in the Immune-active class exhibit a robust and functional immune response characterized by high CTL infiltration. Conversely, patients categorized in the Immune-exclusion class also exhibit a functional immune response, albeit with low CTL infiltration. In contrast, patients classified in the Immune-Dysfunctional class show immune dysfunction despite high CTL infiltration. Finally, patients in the Immune-desert class have both immune dysfunction and low CTL infiltration.

5.4. Differentially expressed genes analyses

All differential gene expression (DEG) analyses were conducted using the R package "limma" [20]. DEGs were identified utilizing the Wilcoxon test, with significance criteria set as absolute log2 (fold change) values greater than 0.5 and *P* values less than 0.05. Volcano plots were generated to visually depict the DEGs between the two groups. These plots provide an intuitive representation of the fold change and statistical significance of gene expression differences, aiding in the identification of genes that are significantly altered between the compared conditions. The use of the Wilcoxon test was preferred due to its robustness in handling non-normally distributed data and its suitability for smaller sample sizes. The choice of an absolute log2 (fold change) threshold greater than 0.5 helps focus on genes with a meaningful change in expression, while the *P* value threshold of less than 0.05 ensures a controlled level of false positives in the analysis.

5.5. Enhancement of functionality

Functional enrichment was employed to assess potential functionalities of the anticipated targets. Gene ontology (GO) is frequently utilized to ascribe roles to genes, covering molecular functions (MF), biological processes (BP), and cellular components (CC). KEGG enrichment offers insights into gene roles and advanced genomic functional data. We utilized the "GOplot" and "clusterProfiler" [21] packages in R to scrutinize the GO roles of expected mRNAs and to amplify KEGG pathways, providing a deeper insight into the oncogenic significance of the target genes. Fisher's exact test was chosen as it is a robust statistical method for analyzing categorical data in small sample sizes, such as gene sets associated with specific functional annotations.

5.6. Identification of the Key Biomarkers

To identify crucial marker genes associated with activated $CD4^+$ memory T cell infiltration and the response to immune checkpoint inhibitors (ICIs), we initiated our investigation by analyzing Differentially Expressed Genes (DEGs) between the high activated $CD4^+$ memory T cell expression group and the low activated $CD4^+$ memory T cell expression group. Additionally, we analyzed DEGs between the reactive and non-reactive groups using data from the IMvigor210 assay. Subsequently, we identified the overlapping genes between these sets of DEGs. To prioritize the importance of each gene, we employed the Random Forest classification algorithm and implemented it using the R software package "randomForest." This method enabled us to rank the genes based on their relevance and association with activated $CD4^+$ memory T cell infiltration and the response to ICIs.

5.7. ICI efficacy Prediction Models constructed with GNN algorithm

To develop a novel model for predicting immune checkpoint inhibitor (ICI) efficacy, we employed deep learning algorithms, with a specific focus on activated $CD4^+$ memory T cells and factors associated with the tumor immune microenvironment (TIME). The IMvigor210 trial data was used as the training group, while the GEO cohort data served as the validation group. The multi-level attention graph neural network (MLA-GNN) [22] was utilized to construct this innovative predictive model.

This approach involved identifying the intersection of differential genes at three key levels: gene expression, activated $CD4^+$ memory T cell infiltration, and factors associated with the TIME. By integrating information from these levels, we aimed to capture a comprehensive view of the intricate interactions in the tumor microenvironment, which can influence ICI response.

To evaluate the performance of our novel model, we utilized the ROC (Receiver Operating Characteristic) function to estimate its accuracy in predicting ICI efficacy. The ROC curve provides a graphical representation of the true positive rate against the false positive rate, enabling a comprehensive assessment of the model's predictive capabilities. A high area under the ROC curve (AUC) would indicate a strong predictive power for ICI response.

5.8. Statistical analysis

Categorical variables were compared using either the chi-square test or Fisher's exact test, depending on the sample size and distribution. For comparisons involving continuous variables, the Mann-Whitney test was employed for two-group comparisons, while the one-way analysis of variance with the Kruskal-Wallis test was utilized for multi-group comparisons. To assess correlation coefficients between variables, Spearman correlation analysis was employed, as it is suitable for non-parametric data. Overall survival (OS) and Progression-Free Survival (PFS) were estimated using the Kaplan-Meier method, and comparisons between survival curves were performed using the log-rank test. For determining optimal cutoff values for continuous variables in each dataset, we employed the R package "survminer". This allowed us to define thresholds that optimize the separation of patient groups based on survival outcomes.

Statistical significance was set at a two-sided P-value less than 0.05, indicating the presence of a statistically significant association or difference. All statistical analyses were performed using R version 4.0.0 (http://www.rproject.org/), a widely used and powerful statistical software environment for bioinformatics and data analysis in the field of oncology and other domains. The choice of R version 4.0.0 was based on its availability at the time of analysis and its compatibility with the necessary packages and functions used in the study.

5.9. Ethics statement

The research methodology was granted ethical approval by the ethics panel at Sun Yat-sen Memorial Hospital, Sun Yat-sen University, Guangzhou, China (Approval Number: SYSEC-KY-KS-2019-171-001). The necessity for informed consent from the subjects under study was exempted by the ethics committee, given that the data were sourced from openly accessible datasets.

Funding

This study was supported by grants 2023YFE0204000 from National Key R&D Program of China, grants 82273204 and 81972471 from the National Natural Science Foundation of China, grant 2023A1515012412 and 2023A1515011214 Guangdong Basic and Applied Basic Research Foundation, grant 2023A03J0722, 202206010078 and 202201020574 from the Guangzhou Science and Technology Project, grant 2018007 from the Sun Yat-Sen University Clinical Research 5010 Program, grant SYS-C-201801 from the Sun Yat-Sen Clinical Research Cultivating Program, grant A2020558 from the Guangdong Medical Science and Technology Program, grant 7670020025 from Tencent CharityFoundation, grant YXQH202209 from the Sun Yat-sen Pilot Scientific Research Fund, and grant HL2021012 from the nursing research project of Sun Yat-Sen Memorial Hospital.

Informed consent statement

Not applicable.

Data availability statement

Publicly available datasets were analyzed in this study. Dataset: IMvigor210 (http://research-pub.gene.com/IMvigor210CoreBiologies/packageVersions/). GEO accession: GSE176307, GSE78220, PRJEB23709, GSE35640 and GSE91061.

CRediT authorship contribution statement

Wenhao Ouyang: Writing – original draft, Methodology. **Qing Peng:** Writing – review & editing, Writing – original draft. **Zijia Lai:** Writing – review & editing, Writing – original draft. **Hong Huang:** Writing – review & editing, Writing – original draft. **Zhenjun Huang:** Methodology. **Xinxin Xie:** Methodology. **Ruichong Lin:** Methodology. **Zehua Wang:** Methodology. **Herui Yao:** Conceptualization. **Yunfang Yu:** Conceptualization.

Declaration of competing interest

The authors declare the following financial interests/personal relationships which may be considered as potential competing interests:Herui Yao reports financial support was provided by National Natural Science Foundation of China. Yunfang Yu reports financial support was provided by Guangdong Basic and Applied Basic Research Foundation. Yunfang Yu reports financial support was provided by Guangzhou Science and Technology Project. Herui Yao reports financial support was provided by Sun Yat-Sen University Clinical Research 5010 Program. Herui Yao reports financial support was provided by Sun Yat-Sen Clinical Research Cultivating Program. Herui Yao reports financial support was provided by Guangdong Medical Science and Technology Program. Herui Yao reports financial support was provided by Tencent CharityFoundation. Yunfang Yu reports financial support was provided by Sun Yat-sen Pilot Scientifc Research Fund. Xinxin Xie reports financial support was provided by nursing research project of Sun Yat-Sen Memorial Hospital. If there are other authors, they declare that they have no known competing financial interests or personal relationships that could have appeared to influence the work reported in this paper.

Acknowledgments

Not applicable.

Appendix A. Supplementary data

Supplementary data to this article can be found online at https://doi.org/10.1016/j.heliyon.2024.e27151.

References

[1] H. Long, Q. Jia, L. Wang, W. Fang, Z. Wang, T. Jiang, F. Zhou, Z. Jin, J. Huang, L. Zhou, C. Hu, X. Wang, J. Zhang, Y. Ba, Y. Gong, X. Zeng, D. Zeng, X. Su, P. B. Alexander, L. Wang, B. Zhu, Tumor-induced erythroid precursor-differentiated myeloid cells mediate immunosuppression and curtail anti-PD-1/PD-L1 treatment efficacy, Cancer Cell 40 (6) (2022) 674–693.e7, https://doi.org/10.1016/j.ccell.2022.04.018.

[2] M.R. Strickland, C. Alvarez-Breckenridge, J.F. Gainor, P.K. Brastianos, Tumor immune microenvironment of brain metastases: toward unlocking antitumor immunity, Cancer Discov. 12 (5) (2022) 1199–1216, https://doi.org/10.1158/2159-8290.CD-21-0976.

[3] C. Li, A.F. Teixeira, H.J. Zhu, P. Ten Dijke, Cancer associated-fibroblast-derived exosomes in cancer progression, Mol. Cancer 20 (1) (2021) 154, https://doi.org/10.1186/s12943-021-01463-y.

[4] S. Wu, H. Huang, R. Sun, D.S. Gao, F. Ye, J. Huang, E. Li, A. Ni, K.G. Lu, K. Chen, J. Jiang, P.A. Morel, Z. Zhong, B. Lu, Synergism between IL21 and anti-PD-1 combination therapy is underpinned by the coordinated reprogramming of the immune cellular network in the tumor microenvironment, Cancer research communications 3 (8) (2023) 1460–1472, https://doi.org/10.1158/2767-9764.CRC-23-0012.

[5] M. Cohen, A. Giladi, O. Barboy, P. Hamon, B. Li, M. Zada, A. Gurevich-Shapiro, C.G. Beccaria, E. David, B.B. Maier, M. Buckup, I. Kamer, A. Deczkowska, J. Le Berichel, J. Bar, M. Iannacone, A. Tanay, M. Merad, I. Amit, The interaction of CD4+ helper T cells with dendritic cells shapes the tumor microenvironment and immune checkpoint blockade response, Nature cancer 3 (3) (2022) 303–317, https://doi.org/10.1038/s43018-022-00338-5.

[6] E.B. Bell, J. Westermann, CD4 memory T cells on trial: immunological memory without a memory T cell, Trends Immunol. 29 (9) (2008) 405–411, https://doi.org/10.1016/j.it.2008.06.002.

[7] G. Betts, E. Jones, S. Junaid, T. El-Shanawany, M. Scurr, P. Mizen, M. Kumar, S. Jones, B. Rees, G. Williams, A. Gallimore, A. Godkin, Suppression of tumour-specific $CD4^+$ T cells by regulatory T cells is associated with progression of human colorectal cancer, Gut 61 (8) (2012) 1163–1171, https://doi.org/10.1136/gutjnl-2011-300970.

[8] F. Wang, J. Long, L. Li, Z.X. Wu, T.T. Da, X.Q. Wang, C. Huang, Y.H. Jiang, X.Q. Yao, H.Q. Ma, Z.X. Lian, Z.B. Zhao, J. Cao, Single-cell and spatial transcriptome analysis reveals the cellular heterogeneity of liver metastatic colorectal cancer, Sci. Adv. 9 (24) (2023) eadf5464, https://doi.org/10.1126/sciadv.adf5464.

[9] D.Y. Oh, S.S. Kwek, S.S. Raju, T. Li, E. McCarthy, E. Chow, D. Aran, A. Ilano, C.S. Pai, C. Rancan, K. Allaire, A. Burra, Y. Sun, M.H. Spitzer, S. Mangul, S. Porten, M.V. Meng, T.W. Friedlander, C.J. Ye, L. Fong, Intratumoral CD4+ T cells mediate anti-tumor cytotoxicity in human bladder cancer, Cell 181 (7) (2020) 1612–1625.e13, https://doi.org/10.1016/j.cell.2020.05.017.

[10] J.R. Veatch, S.M. Lee, C. Shasha, N. Singhi, J.L. Szeto, A.S. Moshiri, T.S. Kim, K. Smythe, P. Kong, M. Fitzgibbon, B. Jesernig, S. Bhatia, S.S. Tykodi, E.T. Hall, D. R. Byrd, J.A. Thompson, V.G. Pillarisetty, T. Duhen, A. McGarry Houghton, E. Newell, S.R. Riddell, Neoantigen-specific CD4+ T cells in human melanoma have diverse differentiation states and correlate with CD8+ T cell, macrophage, and B cell function, Cancer Cell 40 (4) (2022) 393–409.e9, https://doi.org/10.1016/j.ccell.2022.03.006.

[11] L. Zhang, X. Yu, L. Zheng, Y. Zhang, Y. Li, Q. Fang, R. Gao, B. Kang, Q. Zhang, J.Y. Huang, H. Konno, X. Guo, Y. Ye, S. Gao, S. Wang, X. Hu, X. Ren, Z. Shen, W. Ouyang, Z. Zhang, Lineage tracking reveals dynamic relationships of T cells in colorectal cancer, Nature 564 (7735) (2018) 268–272, https://doi.org/10.1038/s41586-018-0694-x.

[12] S. Mariathasan, S.J. Turley, D. Nickles, A. Castiglioni, K. Yuen, Y. Wang, E.E. Kadel III, H. Koeppen, J.L. Astarita, R. Cubas, S. Jhunjhunwala, R. Banchereau, Y. Yang, Y. Guan, C. Chalouni, J. Ziai, Y. Şenbabaoğlu, S. Santoro, D. Sheinson, J. Hung, T. Powles, TGFβ attenuates tumour response to PD-L1 blockade by contributing to exclusion of T cells, Nature 554 (7693) (2018) 544–548, https://doi.org/10.1038/nature25501.
[13] T.L. Rose, W.H. Weir, G.M. Mayhew, Y. Shibata, P. Eulitt, J.M. Uronis, M. Zhou, M. Nielsen, A.B. Smith, M. Woods, M.C. Hayward, A.H. Salazar, M.I. Milowsky, S.E. Wobker, K. McGinty, M.V. Millburn, J.R. Eisner, W.Y. Kim, Fibroblast growth factor receptor 3 alterations and response to immune checkpoint inhibition in metastatic urothelial cancer: a real world experience, Br. J. Cancer 125 (9) (2021) 1251–1260, https://doi.org/10.1038/s41416-021-01488-6.
[14] W. Hugo, J.M. Zaretsky, L. Sun, C. Song, B.H. Moreno, S. Hu-Lieskovan, B. Berent-Maoz, J. Pang, B. Chmielowski, G. Cherry, E. Seja, S. Lomeli, X. Kong, M. C. Kelley, J.A. Sosman, D.B. Johnson, A. Ribas, R.S. Lo, Genomic and transcriptomic features of response to anti-PD-1 therapy in metastatic melanoma, Cell 165 (1) (2016) 35–44, https://doi.org/10.1016/j.cell.2016.02.065.
[15] T.N. Gide, C. Quek, A.M. Menzies, A.T. Tasker, P. Shang, J. Holst, J. Madore, S.Y. Lim, R. Velickovic, M. Wongchenko, Y. Yan, S. Lo, M.S. Carlino, A. Guminski, R.P.M. Saw, A. Pang, H.M. McGuire, U. Palendira, J.F. Thompson, H. Rizos, J.S. Wilmott, Distinct immune cell populations define response to anti-PD-1 monotherapy and anti-PD-1/anti-CTLA-4 combined therapy, Cancer Cell 35 (2) (2019) 238–255.e6, https://doi.org/10.1016/j.ccell.2019.01.003.
[16] A.M. Newman, C.L. Liu, M.R. Green, A.J. Gentles, W. Feng, Y. Xu, C.D. Hoang, M. Diehn, A.A. Alizadeh, Robust enumeration of cell subsets from tissue expression profiles, Nat. Methods 12 (5) (2015) 453–457, https://doi.org/10.1038/nmeth.3337.
[17] H. Cho, F. Tong, S. You, S. Jung, W.H. Kim, J. Kim, Prediction of the immune phenotypes of bladder cancer patients for precision oncology, IEEE open journal of engineering in medicine and biology 3 (2022) 47–57, https://doi.org/10.1109/OJEMB.2022.3163533.
[18] J.E. Rosenberg, J. Hoffman-Censits, T. Powles, M.S. van der Heijden, A.V. Balar, A. Necchi, N. Dawson, P.H. O'Donnell, A. Balmanoukian, Y. Loriot, S. Srinivas, M.M. Retz, P. Grivas, R.W. Joseph, M.D. Galsky, M.T. Fleming, D.P. Petrylak, J.L. Perez-Gracia, H.A. Burris, D. Castellano, R. Dreicer, Atezolizumab in patients with locally advanced and metastatic urothelial carcinoma who have progressed following treatment with platinum-based chemotherapy: a single-arm, multicentre, phase 2 trial, Lancet (London, England) 387 (10031) (2016) 1909–1920, https://doi.org/10.1016/S0140-6736(16)00561-4.
[19] R.S. Herbst, J.C. Soria, M. Kowanetz, G.D. Fine, O. Hamid, M.S. Gordon, J.A. Sosman, D.F. McDermott, J.D. Powderly, S.N. Gettinger, H.E. Kohrt, L. Horn, D. P. Lawrence, S. Rost, M. Leabman, Y. Xiao, A. Mokatrin, H. Koeppen, P.S. Hegde, I. Mellman, F.S. Hodi, Predictive correlates of response to the anti-PD-L1 antibody MPDL3280A in cancer patients, Nature 515 (7528) (2014) 563–567, https://doi.org/10.1038/nature14011.
[20] M.E. Ritchie, B. Phipson, D. Wu, Y. Hu, C.W. Law, W. Shi, G.K. Smyth, Limma powers differential expression analyses for RNA-sequencing and microarray studies, Nucleic Acids Res. 43 (7) (2015) e47, https://doi.org/10.1093/nar/gkv007.
[21] T. Wu, E. Hu, S. Xu, M. Chen, P. Guo, Z. Dai, T. Feng, L. Zhou, W. Tang, L. Zhan, X. Fu, S. Liu, X. Bo, G. Yu, clusterProfiler 4.0: a universal enrichment tool for interpreting omics data, Innovation 2 (3) (2021) 100141, https://doi.org/10.1016/j.xinn.2021.100141.
[22] X. Xing, F. Yang, H. Li, J. Zhang, Y. Zhao, M. Gao, J. Huang, J. Yao, Multi-level attention graph neural network based on co-expression gene modules for disease diagnosis and prognosis, Bioinformatics 38 (8) (2022) 2178–2186, https://doi.org/10.1093/bioinformatics/btac088.
[23] C.L. Gerard, J. Delyon, A. Wicky, K. Homicsko, M.A. Cuendet, O. Michielin, Turning tumors from cold to inflamed to improve immunotherapy response, Cancer Treat Rev. 101 (2021) 102227, https://doi.org/10.1016/j.ctrv.2021.102227.
[24] Y. Yu, W. Zhang, A. Li, Y. Chen, Q. Ou, Z. He, Y. Zhang, R. Liu, H. Yao, E. Song, Association of long noncoding RNA biomarkers with clinical immune subtype and prediction of immunotherapy response in patients with cancer, JAMA Netw. Open 3 (4) (2020) e202149, https://doi.org/10.1001/jamanetworkopen.2020.2149.
[25] N.A. Rizvi, M.D. Hellmann, A. Snyder, P. Kvistborg, V. Makarov, J.J. Havel, W. Lee, J. Yuan, P. Wong, T.S. Ho, M.L. Miller, N. Rekhtman, A.L. Moreira, F. Ibrahim, C. Bruggeman, B. Gasmi, R. Zappasodi, Y. Maeda, C. Sander, E.B. Garon, T.A. Chan, Cancer immunology. Mutational landscape determines sensitivity to PD-1 blockade in non-small cell lung cancer, Science (New York, N.Y.) 348 (6230) (2015) 124–128, https://doi.org/10.1126/science.aaa1348.
[26] J.X. Caushi, J. Zhang, Z. Ji, A. Vaghasia, B. Zhang, E.H. Hsiue, B.J. Mog, W. Hou, S. Justesen, R. Blosser, A. Tam, V. Anagnostou, T.R. Cottrell, H. Guo, H. Y. Chan, D. Singh, S. Thapa, A.G. Dykema, P. Burman, B. Choudhury, K.N. Smith, Transcriptional programs of neoantigen-specific TIL in anti-PD-1-treated lung cancers, Nature 596 (7870) (2021) 126–132, https://doi.org/10.1038/s41586-021-03752-4.
[27] H. Li, A.M. van der Leun, I. Yofe, Y. Lubling, D. Gelbard-Solodkin, A.C.J. van Akkooi, M. van den Braber, E.A. Rozeman, J.B.A.G. Haanen, C.U. Blank, H. M. Horlings, E. David, Y. Baran, A. Bercovich, A. Lifshitz, T.N. Schumacher, A. Tanay, I. Amit, Dysfunctional CD8 T cells form a proliferative, dynamically regulated compartment within human melanoma, Cell 176 (4) (2019) 775–789.e18, https://doi.org/10.1016/j.cell.2018.11.043.
[28] Y. Simoni, E. Becht, M. Fehlings, C.Y. Loh, S.L. Koo, K.W.W. Teng, J.P.S. Yeong, R. Nahar, T. Zhang, H. Kared, K. Duan, N. Ang, M. Poidinger, Y.Y. Lee, A. Larbi, A.J. Khng, E. Tan, C. Fu, R. Mathew, M. Teo, E.W. Newell, Bystander CD8+ T cells are abundant and phenotypically distinct in human tumour infiltrates, Nature 557 (7706) (2018) 575–579, https://doi.org/10.1038/s41586-018-0130-2.
[29] N. Chaput, P. Lepage, C. Coutzac, E. Soularue, K. Le Roux, C. Monot, L. Boselli, E. Routier, L. Cassard, M. Collins, T. Vaysse, L. Marthey, A. Eggermont, V. Asvatourian, E. Lanoy, C. Mateus, C. Robert, F. Carbonnel, Baseline gut microbiota predicts clinical response and colitis in metastatic melanoma patients treated with ipilimumab, Ann. Oncol. : official journal of the European Society for Medical Oncology 28 (6) (2017) 1368–1379, https://doi.org/10.1093/annonc/mdx108.
[30] D.Y. Oh, L. Fong, Cytotoxic CD4+ T cells in cancer: expanding the immune effector toolbox, Immunity 54 (12) (2021) 2701–2711, https://doi.org/10.1016/j.immuni.2021.11.015.
[31] T. Dileepan, D. Malhotra, D.I. Kotov, E.M. Kolawole, P.D. Krueger, B.D. Evavold, M.K. Jenkins, MHC class II tetramers engineered for enhanced binding to CD4 improve detection of antigen-specific T cells, Nat. Biotechnol. 39 (8) (2021) 943–948, https://doi.org/10.1038/s41587-021-00893-9.
[32] M. Künzli, D. Masopust, CD4+ T cell memory, Nat. Immunol. 24 (6) (2023) 903–914, https://doi.org/10.1038/s41590-023-01510-4.
[33] T. Ahrends, J. Borst, The opposing roles of CD4+ T cells in anti-tumour immunity, Immunology 154 (4) (2018) 582–592, https://doi.org/10.1111/imm.12941. Advance online publication.
[34] B.A. Helmink, S.M. Reddy, J. Gao, S. Zhang, R. Basar, R. Thakur, K. Yizhak, M. Sade-Feldman, J. Blando, G. Han, V. Gopalakrishnan, Y. Xi, H. Zhao, R.N. Amaria, H.A. Tawbi, A.P. Cogdill, W. Liu, V.S. LeBleu, F.G. Kugeratski, S. Patel, J.A. Wargo, B cells and tertiary lymphoid structures promote immunotherapy response, Nature 577 (7791) (2020) 549–555, https://doi.org/10.1038/s41586-019-1922-8.
[35] P. Voabil, M. de Bruijn, L.M. Roelofsen, S.H. Hendriks, S. Brokamp, M. van den Braber, A. Broeks, J. Sanders, P. Herzig, A. Zippelius, C.U. Blank, K.J. Hartemink, K. Monkhorst, J.B.A.G. Haanen, T.N. Schumacher, D.S. Thommen, An ex vivo tumor fragment platform to dissect response to PD-1 blockade in cancer, Nat. Med. 27 (7) (2021) 1250–1261, https://doi.org/10.1038/s41591-021-01398-3.
[36] Y. Zhang, H. Chen, H. Mo, X. Hu, R. Gao, Y. Zhao, B. Liu, L. Niu, X. Sun, X. Yu, Y. Wang, Q. Chang, T. Gong, X. Guan, T. Hu, T. Qian, B. Xu, F. Ma, Z. Zhang, Z. Liu, Single-cell analyses reveal key immune cell subsets associated with response to PD-L1 blockade in triple-negative breast cancer, Cancer Cell 39 (12) (2021) 1578–1593.e8, https://doi.org/10.1016/j.ccell.2021.09.010.
[37] M. Yang, J. Lu, G. Zhang, Y. Wang, M. He, Q. Xu, C. Xu, H. Liu, CXCL13 shapes immunoactive tumor microenvironment and enhances the efficacy of PD-1 checkpoint blockade in high-grade serous ovarian cancer, Journal for immunotherapy of cancer 9 (1) (2021) e001136, https://doi.org/10.1136/jitc-2020-001136.
[38] H.W. Lim, C.H. Kim, Loss of IL-7 receptor alpha on CD4+ T cells defines terminally differentiated B cell-helping effector T cells in a B cell-rich lymphoid tissue, J. Immunol. 179 (11) (2007) 7448–7456, https://doi.org/10.4049/jimmunol.179.11.7448.
[39] S. Hong, Y. Zhang, M. Cao, A. Lin, Q. Yang, J. Zhang, P. Luo, L. Guo, Hypoxic characteristic genes predict response to immunotherapy for urothelial carcinoma, Front. Cell Dev. Biol. 9 (2021) 762478, https://doi.org/10.3389/fcell.2021.762478.
[40] J. Qiu, X. Li, Y. He, Q. Wang, J. Li, J. Wu, Y. Jiang, J. Han, Identification of comutation in signaling pathways to predict the clinical outcomes of immunotherapy, J. Transl. Med. 20 (1) (2022) 613, https://doi.org/10.1186/s12967-022-03836-3.
[41] Y. Wang, L. Chen, M. Yu, Y. Fang, K. Qian, G. Wang, L. Ju, Y. Xiao, X. Wang, Immune-related signature predicts the prognosis and immunotherapy benefit in bladder cancer, Cancer Med. 9 (20) (2020) 7729–7741, https://doi.org/10.1002/cam4.3400.
[42] Y. Xu, T. Tao, S. Li, S. Tan, H. Liu, X. Zhu, Prognostic model and immunotherapy prediction based on molecular chaperone-related lncRNAs in lung adenocarcinoma, Front. Genet. 13 (2022) 975905, https://doi.org/10.3389/fgene.2022.975905.

[43] Q. Wang, Y. Chen, W. Gao, H. Feng, B. Zhang, H. Wang, H. Lu, Y. Tan, Y. Dong, M. Xu, Identification and validation of a four-gene ferroptosis signature for predicting overall survival of lung squamous cell carcinoma, Front. Oncol. 12 (2022) 933925, https://doi.org/10.3389/fonc.2022.933925.

[44] L. Wang, S. Zhang, H. Li, Y. Xu, Q. Wu, J. Shen, T. Li, Y. Xu, Quantification of m6A RNA methylation modulators pattern was a potential biomarker for prognosis and associated with tumor immune microenvironment of pancreatic adenocarcinoma, BMC Cancer 21 (1) (2021) 876, https://doi.org/10.1186/s12885-021-08550-9.

[45] J.N. Kather, L.R. Heij, H.I. Grabsch, C. Loeffler, A. Echle, H.S. Muti, J. Krause, J.M. Niehues, K.A.J. Sommer, P. Bankhead, L.F.S. Kooreman, J.J. Schulte, N. A. Cipriani, R.D. Buelow, P. Boor, N.N. Ortiz-Brüchle, A.M. Hanby, V. Speirs, S. Kochanny, A. Patnaik, T. Luedde, Pan-cancer image-based detection of clinically actionable genetic alterations, Nature cancer 1 (8) (2020) 789–799, https://doi.org/10.1038/s43018-020-0087-6.

[46] J.Y. Shi, X. Wang, G.Y. Ding, Z. Dong, J. Han, Z. Guan, L.J. Ma, Y. Zheng, L. Zhang, G.Z. Yu, X.Y. Wang, Z.B. Ding, A.W. Ke, H. Yang, L. Wang, L. Ai, Y. Cao, J. Zhou, J. Fan, X. Liu, Q. Gao, Exploring prognostic indicators in the pathological images of hepatocellular carcinoma based on deep learning, Gut 70 (5) (2021) 951–961, https://doi.org/10.1136/gutjnl-2020-320930.